Chemie der Erde 75 (2015) 287–300

Contents lists available at ScienceDirect

Chemie der Erde

journal homepage: www.elsevier.de/chemer

Chemical and isotopic characteristics and origin of spring waters in the Lanping–Simao Basin, Yunnan, Southwestern China

Ying Bo[a,b,*], Chenglin Liu[a,b,*], Yanjun Zhao[b], Licheng Wang[b]

[a] MLR Key Laboratory of Metallogeny and Mineral Assessment, Institute of Mineral Resources, Chinese Academy of Geological Sciences, 100037 Beijing, China
[b] Institute of Mineral Resources, Chinese Academy of Geological Sciences, 100037 Beijing, China

ARTICLE INFO

Article history:
Received 13 October 2014
Accepted 12 April 2015
Editorial handling - H. Guo

Keywords:
Spring
Hydrochemistry
Reservoir temperature
Isotope
Evolution
Lanping–Simao

ABSTRACT

The chemical and isotopic characteristics (oxygen, hydrogen, and strontium) of spring waters and isotopic compositions of helium (He) and neon (Ne) in gases escaping from spring waters in the Lanping–Simao Basin are studied. A total of twenty-one spring water samples (twelve hot springs, four cold springs, and five saline springs) and eleven gas samples were collected from the study area, including one spring and one gas sample from northern Laos. It is found that saline spring waters in the study area are of chloride type, cold spring waters are of carbonate type or sulfate type, and hot spring waters are of various types. High total dissolved solids levels in saline springs are significantly related to Upper Cretaceous–Paleocene salt-bearing strata. On the basis of hydrochemical geothermometry, the reservoir temperatures (T_r) for hot springs, cold springs, and saline springs are 65.5–144.1, 37.8–64.4, and 65.1–109.0 °C, respectively, and the circulation depths of saline springs are much larger than those of hot and cold springs. The oxygen and hydrogen isotopic compositions of springs in the Lanping–Simao Basin and northern Laos are primarily controlled by meteoric waters with obvious latitude and altitude effects, and are also influenced by $\delta^{18}O$ exchange to some extent. Most Sr^{2+} in spring waters of the study area is derived from varied sources (carbonate, evaporite, and silicate mineral dissolution), and the Sr isotopic compositions are greatly influenced by volcanic rocks. Wide distribution of crust-derived He in the Lanping–Simao Basin and northern Laos reveal that faults in these areas may not descend to the upper mantle. It is concluded that water circulation in the study area may be limited above the upper mantle, while saline springs may originate from the Upper Cretaceous–Paleocene evaporites. Hydrochemical characteristics demonstrate affinities among the Lanping–Simao Basin, northern Laos, and Yanjing, eastern Tibet, while disaffinities are observed between these areas and Tengchong on the basis of the hydrochemical characteristics and noble gas isotopic compositions.

1. Introduction

Yunnan Province is located in Southwestern China, and contains more than one thousand springs, accounting for almost one-third of all springs in China. In recent decades, Rehai, Tengchong County, the volcano–geothermal region in western Yunnan, has caused concern to many geologists and geochemists (Zhang et al., 1989; Gao and Fan, 1992; Zhao et al., 2006; Zhao, 2008; Liu et al., 2009), because of the dense distribution of thermal springs and the development of fault belts. Our study area, the Lanping–Simao Basin (LP–SM) (Fig. 1), lies in central-south Yunnan and to the east of Tengchong County, where geothermal activity and faults also occur. The basin is rich in various types of metallic and nonmetallic mineral resources, with an ultra-large Pb–Zn ore deposit (the Jinding Pb–Zn Ore Deposit) in Lanping County and a small potash ore deposit (the Mengyejing Potash Deposit) in Jiangcheng County (Fig. 1 and Fig. 3). As a saline basin, the Lanping–Simao Basin is famous for the Mengyejing Potash Deposit, which is to date the only solid potash deposit discovered in China. Thus, the geological and tectonic evolution of the basin has been the focus of a large amount of research (Guo, 1986; Yin, 1990; Zhu et al., 1997; Qu, 1997; Zhou et al., 2001). However, the hydrochemistry of spring waters in the Lanping–Simao Basin has rarely been described, except for the ion concentrations and ion ratios of saline springs studied for potash deposit prospecting in the 1970s (Scientific Research Team for Potash Geology of Yunnan Geology Bureau, 1979).

* Corresponding authors at: 26 Baiwanzhuang Street, Xicheng District, 100037 Beijing, China. Tel.: +86 010 68999067; fax: +86 010 68327263.
E-mail addresses: sunnybritney@hotmail.com (Y. Bo), liuchengl@263.net (C. Liu).

http://dx.doi.org/10.1016/j.chemer.2015.04.002
0009-2819/

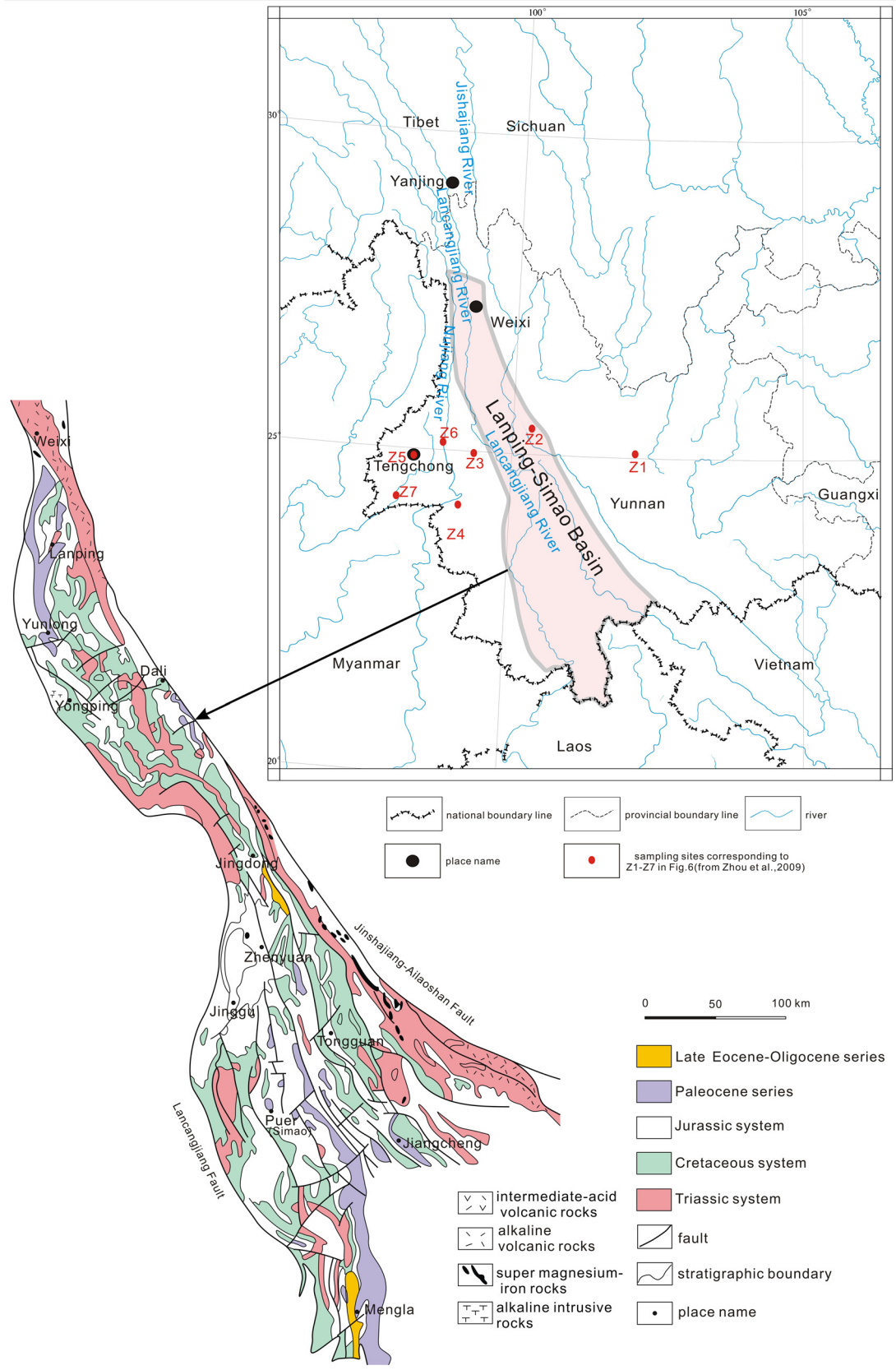

Fig. 1. Position and geologic sketch map of the study area. The base map of the Lanping–Simao Basin is modified from Qu et al. (1998).

Hydrochemical and isotopic characteristics of springs are of great importance for understanding the water circulation and evolution (e.g., material source and recharge source of water) of a saline basin, which are sometimes related to the formation of metallic and nonmetallic ore deposits (Tornos and Heinrich, 2008; Cao et al., 2010; Bo et al., 2013). In addition, thermal springs have been used for bathing and balneological purposes by local residents for many years. Therefore, there is a need for detailed study of the geochemical and isotopic characteristics of spring waters in this area.

This study addresses the chemical and isotopic characteristics of spring waters as well as isotopic compositions of He and Ne in gases escaping from spring waters in the Lanping–Simao Basin. For comparison, hot springs from the surrounding area (Rehai, Tengchong County, Yanjing Town, eastern Tibet, and Muangla, northern Laos) are also referred in this study (Fig. 1). These three regions are located in the Tengchong Terrane, the Changdu Block, and the Indo-China Terrane, respectively (He et al., 2011; Metcalfe, 2013). In addition, the Changdu Block, the Lanping–Simao Basin, and the Indo-China Terrane are arranged successively from north to south in the same tectonic belt.

2. Geological and physical setting

The Lanping–Simao Basin is located in the southern section of the Sanjiang fold system in western Yunnan, stretching along a NW–SE direction from northern Weixi in the north to northern Vietnam and northern Laos in the south, and from the Lancangjiang deep fault in the west to the Jinshajiang-Ailaoshan deep fault in the east (Fig. 1). Along the Lancangjiang River and the Honghe Valley, the Lancangjiang deep fault with a length of 800 km extends northwardly into Tibet and to the Thailand-Laos boarder southwardly. Being the western boundary of the Lanping–Simao Basin, the Lancangjiang deep fault has taken a significant control on its magmatism, sedimentation and metamorphism since the Mesozoic. The Jinshajiang-Ailaoshan fault extends into western Sichuan along the Jinshajiang River to the north and Vietnam along the west slope of the Ailaoshan Mountain to the south, and the middle part of the fault is destroyed by the Qiaohou fault and the Honghe fault. As a suture during the Late Variscan, the Jinshajiang-Ailaoshan fault has been reactivated as well as a basin-controlling fault on the east of the Lanping–Simao Basin since the Mesozoic.

The basin is narrower in the north and wider in the south, and is divided into two parts with Jingdong, the narrowest part in the middle. The southern part of the basin is called the Simao Subbasin, and the northern part is called the Lanping Subbasin (Sun and Sun, 1990). The Lanping–Simao Basin is an intracontinental polycyclic superimposed basin that has developed since the Middle Triassic Epoch. The formation and evolution of the basin are thought to have been closely related to deep processes (Yin, 1990). The basin has experienced complex tectonic evolution: from a continental rift basin (T_3–J_1) to a depression basin (J_2–K_1) to a foreland basin (K) to a strike-slip basin (E) (Qian et al., 1994), with very thick Mesozoic and Cenozoic sedimentary rocks developed and Paleogene strata sporadically cropping out from Lanping to Yunlong. The Jurassic–Eocene (J–E_2) strata are characterized by red beds with interbedded evaporites (Qu et al., 1998), and Upper Cretaceous–Paleocene salt-bearing deposits are widely distributed in the basin (Fig. 1). In addition, volcanic rocks are well developed in the Devonian–Triassic sequence, silicate rocks are developed in the Carboniferous–Triassic strata, and carbonate rocks are primarily distributed in the Devonian and Triassic strata (Fig. 2) (Qu et al., 1998).

Tengchong is famous not only for modern volcanic activity but also as an area of geothermal anomalies. The Tengchong Block is characterized by carbonate rocks developed in the Devonian to Triassic to strata and oceanic crust (basalts) developed in the Cambrian to Paleogene strata (Qu et al., 1998). Yanjing Town, eastern Tibet, is located immediately to the north of the Lanping–Simao Basin, which is also related to the Sanjiang Fold System.

Lying in a low-latitude mountainous highland with altitudes ranging from 317 m at the Tuka estuary (Bao and Qiu, 2007) to 4435.4 m at the summit of Laowo Mountain (Lanping Bai and Pumi Autonomous County Party Committee and Government, 2005), the basin shows obvious regional and vertical differences of climate. The annual temperature ranges from 13.7 to 20.2 °C (Bao and Qiu, 2007; Lanping Bai and Pumi Autonomous County Party Committee and Government, 2005). The basin is characterized by plentiful rainfall and abundant rivers; the annual mean rainfall is 1100 mm, and even as much as 1600 mm in the southern part of the basin. As a result of the influence of the southwest monsoon, the summers are hot and humid with abundant rainfall (from June to August) and the winters and springs are dry (from November to April).

3. Materials and methods

A total of 21 spring samples (including one from Muangla, northern Laos, sample No. 21) were collected between April 18 and May 3, 2012, during our field investigations in the Lanping–Simao Basin and northern Laos. The sampling sites are marked in Fig. 3.

Sampling was done in accordance with the relevant operation guides (MGMR, 1987; EPA, 2004). After being filtered through 0.45 μm filter paper, water from a sampling site was transferred into two low-density polyethylene bottles for cation (acidified with HNO_3 to a final concentration of 5%) and anion (without adding any reagent) analysis. Water samples for oxygen, hydrogen, and strontium isotope analysis were collected in inclosed high-density polyethylene bottles without addition of any reagent. During sampling, pH values were measured with a portable pH meter. Gas samples were collected from spring waters (0.1–1.0 m underwater) by displacement of saturated NaCl solution using a set of specially made sampling devices and then sealed in 250-ml glass bottles (inverted, with about 80 ml of saturated NaCl solution retained).

Water samples were sent to the National Research Center for Geoanalysis (NRCGA, PRC) for chemical analysis. K^+, Ca^{2+}, Na^+, and Mg^{2+} were determined by inductively coupled plasma and atomic emission spectrometry (ICP-AES, IRIS Advantage, Thermo Jarrell Ash, USA); Cl^-, HCO_3^-, and CO_3^{2-} were measured using the volumetric method; SO_4^{2-} was measured using the gravimetric method (CO_3^{2-} was undetected). Minor ions, such as Si (SiO_2), Sr^{2+}, Li^+, B^{3+}, Br^-, and I^-, were measured by inductively coupled plasma and mass spectrometry (ICP-MS, Agilent 7500a, Agilent, USA). Cl^- and SO_4^{2-} were also detected by ion chromatography (Dionex ICS900, USA). Br^-, I^-, and B^{3+} (expressed as B_2O_3) were measured using colorimetry. More details of sample analysis and quality control can be found in Bo et al. (2013).

The oxygen and hydrogen isotope compositions were determined using standard methods for water (Epstein and Mayeda, 1953; Coleman et al., 1982). The analytical precision for oxygen and hydrogen determinations is ±0.2‰ and 2‰ (MAT 253 stable isotope ratio mass spectrometer, Thermo Scientific, USA), respectively. The strontium isotope composition was measured using a Thermo Ionization Mass Spectrometer MAT262 (Finnigan GmbH, Germany), with the standard analytical result of NBS987$SrCO_3$ $^{87}Sr/^{86}Sr = 0.710247 \pm 12$ (2σ), and mass fractionation was corrected using $^{87}Sr/^{86}Sr = 0.837521$.

Gas samples were sent to the Key Laboratory of Gas Geochemistry, Chinese Academy of Sciences (Lanzhou, China), immediately after they were collected; the determination of the samples was completed in 30 days. The helium and neon contents were determined using an MAT 271 mass spectrometer (Finnigan GmbH, Germany) by comparing the peak intensity between ^4He and ^{20}Ne of air (AIRLZ2007: $^4He = 2.46 \times 10^{-10}$ cm^3STP/g and $^{20}Ne = 4.08 \times 10^{-10}$ cm^3STP/g) and those of the gas sample, with the absolute deviation (AD) within 10%. Analyses of the helium and neon isotopes were conducted using a static vacuum mass spectrometer (MM5400, Micromass, UK). More details on helium and neon isotope analysis are given in Ye et al. (2007).

4. Results

4.1. Hydrochemical features of spring waters

Chemical and isotopic data of spring waters from the Lanping–Simao Basin and northern Laos are listed in Table 1. From the outlet temperature (T_{spring}) and total dissolved solids (TDS), the 21 water samples are divided into three groups: hot springs ($T_{spring} > 20$ °C), cold springs ($T_{spring} \leq 20$ °C, TDS < 10 g/L), and saline

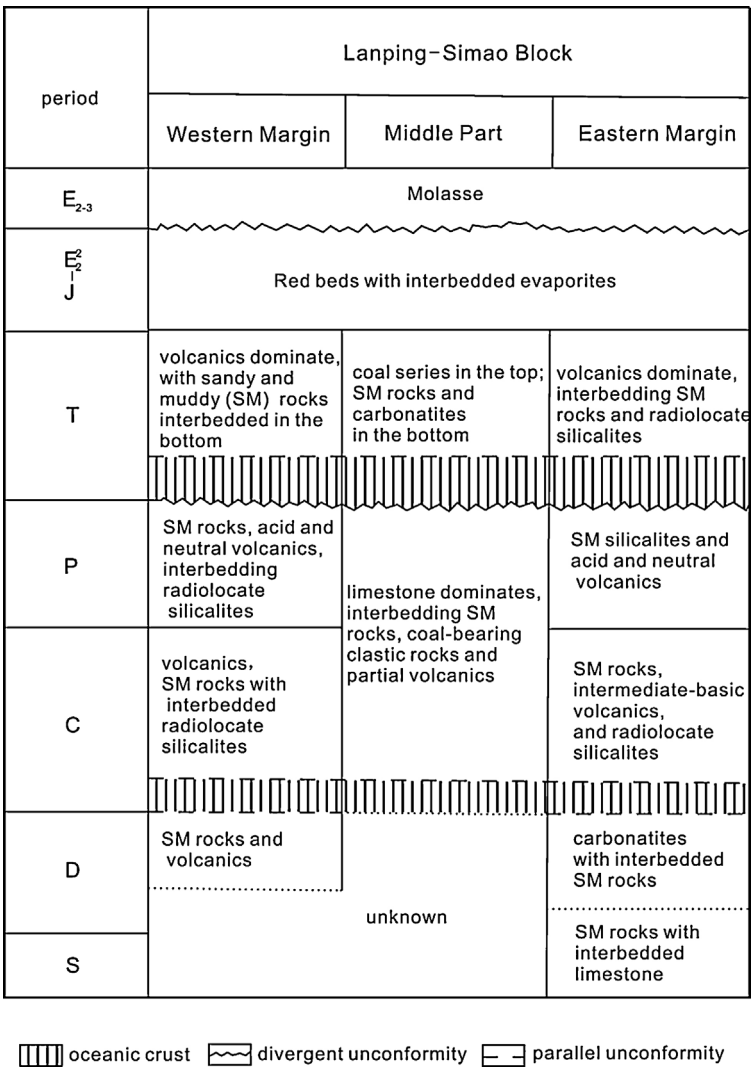

Fig. 2. Tectonic foundation and sedimentary formation of the Lanping–Simao Basin. According to Qu et al. (1998).

springs ($T_{spring} \leq 20\,^{\circ}C$, TDS > 10 g/L). The TDS of saline springs, hot springs, and cold springs are 37.238–300.475, 0.515–10.064 and 0.071–0.271 g/L, respectively, and the pH values are 6.13–7.47, 7.26–8.05, and 7.47–7.66, respectively (Table 1).

As listed in Table 1, on the basis of Schukalev's classification and Kurllov's formula (MGMR, 1983), saline spring waters are of Na–Cl type; hot spring waters are of various types, from Na–HCO_3 to Na–Ca–SO_4–HCO_3 to Na–Cl–HCO_3–SO_4 to Na–Ca–SO_4–Cl to Na–Cl type; cold spring waters are of Ca–Mg–HCO_3 type or Ca–HCO_3 type.

According to the classification of Valyashko (1965), all five saline spring samples are of chloride type. Five hot spring samples are of carbonate type, three (including No. 21) are chloride type, three are sodium sulfate subtype, and only one is magnesium sulfate subtype. The four cold spring samples are of carbonate type (one), sodium sulfate type (one), and magnesium sulfate type (two).

The hot springs of Rehai ($n = 8$) are of carbonate type, with TDS values ranging from 0.48 to 2.81 g/L, pH values from 4.2 to 9.6, and temperatures from 73 to 94 °C (Zhang et al., 1989). The hot springs of Yanjing ($n = 13$) mainly belong to the chloride type, with TDS values of 25.907–86.656 g/L, pH 6.3–6.7, and temperatures 24.5–62.5 °C (Qian, 2007).

Figs. 4 and 5 show the concentrations of major and minor ions in springs from the study area (including one from northern Laos), and Fig. 4 also shows those of representative hot spring waters from Rehai, Tengchong, and Yanjing, eastern Tibet. The saline spring waters in the Lanping–Simao Basin have similar chemical characteristics, with Na + K > Ca > Mg and Cl > SO_4 > HCO_3 chemical compositions (Fig. 5); in the Piper diagram (Fig. 4), the data points for the cations and anions fall near to the Na-end-member (Na + K) and the Cl-end-member, respectively. The compositions of cold springs are relatively consistent, with Ca^{2+} and Mg^{2+} as the main cations (Ca > Mg > Na + K) and HCO_3^- as the main anion (HCO_3 > SO_4 > Cl or HCO_3 > Cl > SO_4). For hot springs in the Lanping–Simao Basin and northern Laos, Na^+ is the main cation (Na + K > Ca > Mg), accounting for 49%–89% of the total cations, and SO_4^{2-} or Cl^- are the main anions (except for Nos. 3, 4, and 5).

From Fig. 4, the chemical compositions of saline springs and most hot springs (except Nos. 3, 4, and 5) of the Lanping–Simao Basin are similar to the hot springs of northern Laos and Yanjing but quite different from those of Rehai.

4.2. Hydrochemical geothermometry

There are four frequently-used chemical geothermometers: the silica geothermometer, Na/K geothermometer, Na–K–Ca geothermometer, and K/Mg geothermometer. Truesdell (1975) and Fournier (1979) each proposed two Na/K geothermometers, Fournier (1981) proposed six silica geothermometers and one

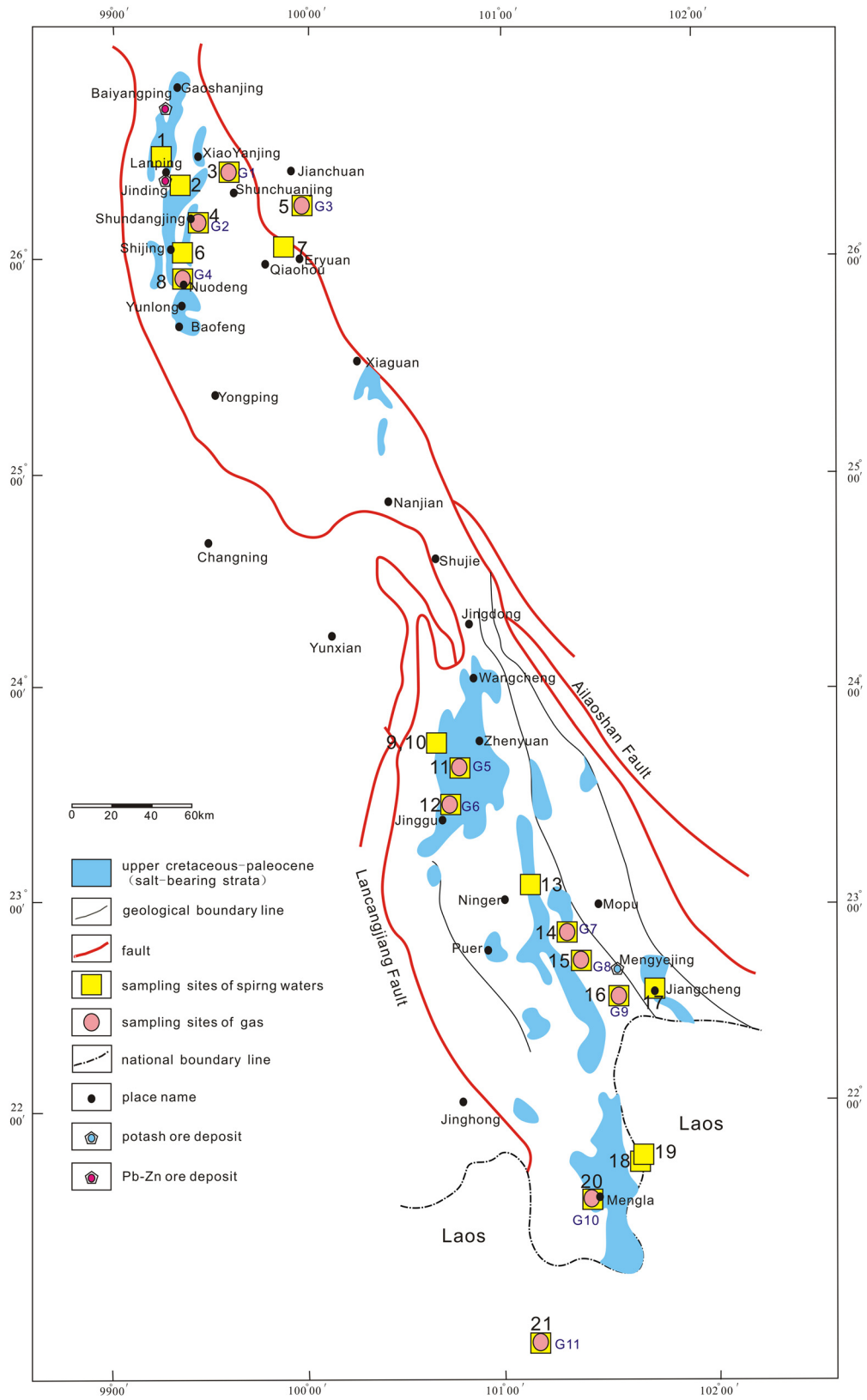

Fig. 3. Sampling sites in the Lanping–Simao Basin and northern Laos. The base map is from 814 Geological Team, Yunnan Bureau of Geology and Mineral Resources, (1994).

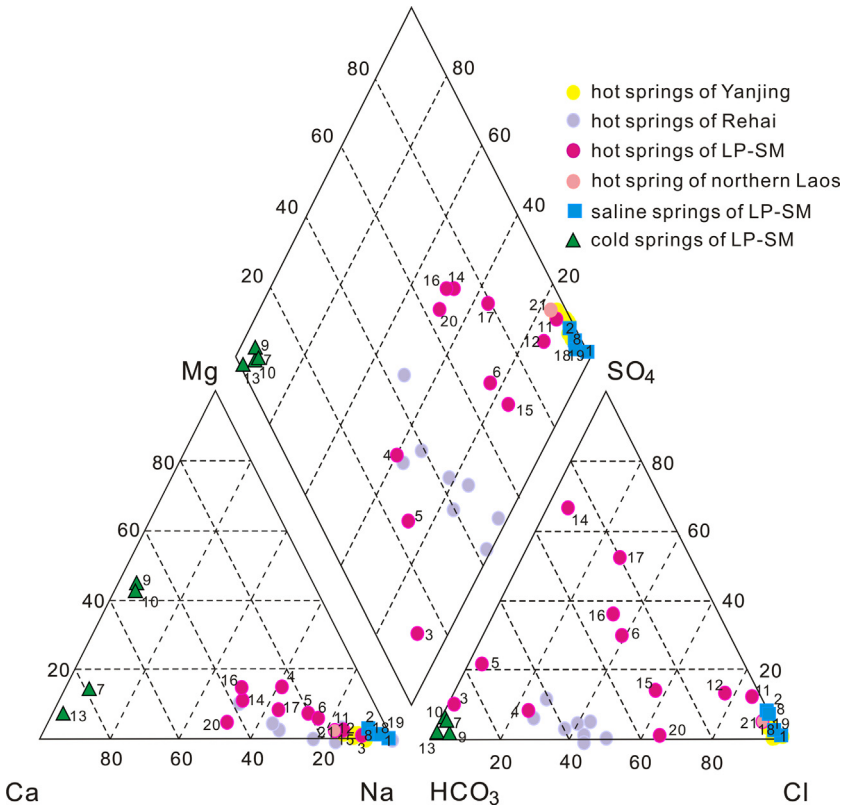

Fig. 4. Piper diagram of spring waters from the Lanping–Simao Basin, northern Laos, Rehai, and Yanjing. Data points of the Lanping–Simao Basin and northern Laos correspond to numbers in Fig. 3 and Table 1; LP–SM indicates the Lanping–Simao Basin. This notation is the same in the other figures.

Na–K–Ca geothermometer, Rybach and Muffler (1981) proposed one silica geothermometer, one Na/K geothermometer, and one Na–K–Ca geothermometer, and Giggenbach (1988) proposed one K/Mg geothermometer. Four representative formulas for reservoir temperature (θ) estimation suggested by Fournier (1981) (Eqs. (A.1)–(A.3)) and Giggenbach (1988) (Eq. (A.4)) are as follows:

$$\theta_{SiO_2}\ (^\circ C) = \frac{1309}{5.19 - \log\ SiO_2} - 273.15 \quad (A.1)$$

$$\theta_{Na/K}\ (^\circ C) = \frac{1217}{\log(Na/K) + 1.483} - 273.15 \quad (A.2)$$

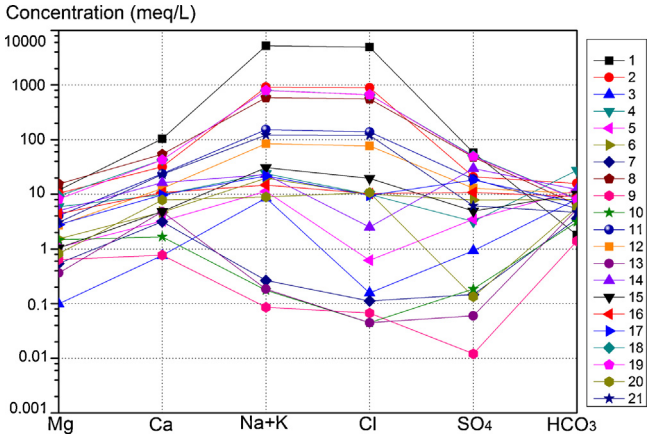

Fig. 5. Schoeller semi-logarithmic diagram of waters from the Lanping–Simao Basin and northern Laos.

$$\theta_{NaKCa}\ (^\circ C) = \frac{1647}{\log(Na/K) + \beta\left[(\log\sqrt{Ca}/Na) + 2.06\right] + 2.47} - 273.15 \quad (A.3)$$

First take $\beta = 4/3$, and if the calculated $\theta_{NaKCa} > 100$ or $(\log\sqrt{Ca}/Na) + 2.06 < 0$, then change the β value from 4/3 to 1/3.

$$\theta_{KMg}\ (^\circ C) = \frac{4410}{13.95 - \log(K^2/Mg)} - 273.15 \quad (A.4)$$

However, all these geothermometers use the common assumption that waters are fully equilibrated. In addition, different geothermometers have their own restrictive conditions or defects, for instance, dilution of cold water has an obvious effect on the calculation of the Na–K–Ca geothermometer. Thus, methods and rules were suggested by Brook et al. (1979), Fournier (1981), and Tong and Zhang (1989) to choose the calculated credible reservoir temperature (T_r) among those estimated temperatures (Zhao, 2008):

If $\theta_{NaK} > \theta_{SiO_2} > \theta_{NaKCa}$, then $T_r = \theta_{SiO_2}$;

If $\theta_{NaKCa} > \theta_{NaK}$, then $T_r = \theta_{SiO_2}$;

If $\theta_{NaK} > \theta_{NaKCa} > \theta_{SiO_2} > \theta_{KMg}$, then $T_r = \theta_{SiO_2}$;

If $\theta_{SiO_2} > \theta_{NaK} > \theta_{NaKCa} > \theta_{KMg}$, then $T_r = \theta_{NaK}$;

If $\theta_{SiO_2} > \theta_{NaK} > \theta_{KMg} > \theta_{NaKCa}$, then $T_r = \theta_{NaK}$;

If $\theta_{NaK} > \theta_{NaKCa} > \theta_{KMg} > \theta_{SiO_2}$ and $T_{spring} < 40\ ^\circ C$, then $T_r = \theta_{NaKCa}$;

Table 1
Chemical and isotopic data of spring waters in the Lanping–Simao Basin and northern Laos.

Sample No.	Sample type	Sampling site	TDS (g/L)	pH	T_{spring}[a] (°C)	T_r[b] (°C)	K (mg/L)	Na (mg/L)	Ca (mg/L)	Mg (mg/L)	Cl (mg/L)	SO_4^{2-} (mg/L)	HCO_3^- (mg/L)
1	Saline spring	Lajing Town, Lanping	300.475	6.13	<20	109.0	220.0	120,600.0	2083.0	142.0	174,603.0	2772.0	110.0
2	Saline spring	Qingmen village, Qingmen	55.121	7.47	<20	95.1	223.0	20,910.0	637.0	125.0	31,746.0	999.0	961.0
3	hot Spring	Xinhe Village, Jianchuan	0.515	8.05	51	136.0	8.1	191.0	15.4	1.2	5.6	44.8	498.0
4	Hot spring	Dalong Village, Yunlong	2.181	7.44	40	98.3	51.8	519.0	197.0	70.9	353.0	152.0	1674.0
5	Hot spring	Niujie Village, Eryuan	0.904	7.75	81	144.1	33.3	242.0	64.6	12.9	22.2	167.0	723.0
6	Hot spring	Hekou Spring, Yunlong	1.549	8.01	50	–	8.5	449.0	94.3	18.5	357.0	377.0	489.0
7	Cold spring	Longmen Village, Jianchuan	0.197	7.56	<20	56.4	1.8	5.1	62.8	6.6	4.0	7.0	219.0
8	Saline spring	Nuodeng Village, Yunlong	37.238	7.19	<20	82.5	158.0	13,480.0	1079.0	186.0	19,841.0	2298.0	392.0
9	Cold spring	Dalubian Village, Jinggu	0.071	7.66	<20	43.9	0.9	1.4	15.5	7.7	2.4	0.6	85.6
10	Cold spring	Dalubian Village, Jinggu	0.161	7.52	<20	37.8	1.1	3.4	33.6	17.8	1.6	8.9	189.0
11	Hot spring	Mangka Spring, Jinggu	10.064	7.41	70	97.1	30.7	3511.0	476.0	48.6	4921.0	910.0	333.0
12	Hot spring	South of Jinggu Paper Mill	5.912	7.47	50	102.8	15.9	1941.0	256.0	32.5	2730.0	620.0	633.0
13	Cold spring	Wenquan Village, Ninger	0.271	7.47	20	64.4	0.5	4.0	96.0	4.4	1.6	2.9	324.0
14	Hot spring	Dashujiao Village, Jiangcheng	2.806	7.36	48	109.5	17.0	518.0	326.0	59.6	88.9	1423.0	746.0
15	Hot spring	Mankelao Village, Jiangcheng	2.060	7.58	60	92.3	10.0	704.0	96.7	12.5	694.0	237.0	612.0
16	Hot spring	Zhengdong Town, Jiangcheng	1.767	7.54	40	–	4.6	338.0	214.0	52.8	365.0	518.0	549.0
17	Hot spring	Erguanzhai Village, Jiangcheng	2.162	7.26	35	84.8	9.2	494.0	194.0	33.4	339.0	878.0	429.0
18	Saline spring	Yanjing Village, Mengla	45.725	7.11	<20	66.5	190.0	18,270.0	856.0	111.0	23,611.0	2439.0	495.0
19	Saline spring	Yanjingqing, Mengla	45.488	6.93	<20	65.1	189.0	18,130.0	856.0	98.0	23,611.0	2359.0	489.0
20	Hot spring	Wenquan Village, Mengla	0.937	7.54	40	65.5	5.5	202.0	157.0	9.9	381.0	6.4	351.0
21	Hot spring	Muangla, northern Laos	8.058	7.44	66	95.5	78.4	2756.0	463.0	36.7	4286.0	295.0	285.0

Sample No.	Sample type	Br (mg/L)	B (mg/L)	Sr (mg/L)	Li (mg/L)	I (mg/L)	SiO_2 (mg/L)	$^{87}Sr/^{86}Sr$	δD	$\delta^{18}O$	Water type[c]	Water type[d]
1	Saline spring	18.000	3.070	48.900	0.910	0.170	58.2	0.709793	−106	−14.3	Chloride type	Na–Cl
2	Saline spring	16.100	0.390	8.890	0.096	0.031	43.2	0.709786	−69	−7.6	Chloride type	Na–Cl
3	Hot spring	0.110	0.340	0.350	0.330	0.002	97.9	0.714869	−122	−15.3	Carbonate type	Na–HCO_3
4	Hot spring	0.120	3.890	0.990	1.390	0.008	46.3	0.713439	−113	−13.8	Carbonate type	Na–HCO_3
5	Hot spring	0.090	2.850	1.250	1.310	0.023	113	0.708583	−116	−12.8	Carbonate type	Na–HCO_3
6	Hot spring	0.190	0.710	1.340	0.240	0.007	56.2	0.712743	−110	−12.8	Carbonate type	Na–Cl–HCO_3–SO_4
7	Cold spring	<0.05	<0.02	0.590	0.002	0.001	16.5	0.708037	−98	−12.3	Magnesium sulfate subtype	Ca–HCO_3
8	Saline spring	6.220	1.520	15.800	0.140	0.021	32.3	0.709428	−97	−11.8	Chloride type	Na–Cl
9	Cold spring	<0.05	<0.02	0.042	0.002	0.003	11.5	0.710817	−71	−9.2	Magnesium sulfate subtype	Ca–Mg–HCO_3
10	Cold spring	<0.05	0.020	0.130	0.004	<0.001	9.56	0.710252	−74	−9.3	Sodium sulfate subtype	Ca–Mg–HCO_3
11	Hot spring	2.800	1.390	12.400	0.800	0.010	45.1	0.709951	−86	−11.1	Chloride type	Na–Cl
12	Hot spring	0.950	0.840	6.120	0.310	0.008	51.1	0.70958	−86	−10.9	Sodium sulfate subtype	Na–Cl
13	Cold spring	<0.05	<0.02	0.280	0.003	0.001	20.5	0.707849	−71	−9.1	Carbonate type	Ca–HCO_3
14	Hot spring	0.070	0.470	2.940	0.096	0.004	58.8	0.713592	−83	−10.4	Sodium sulfate subtype	Na–Ca–SO_4–HCO_3
15	Hot spring	0.330	0.660	1.600	0.140	0.008	57.5	0.710673	−75	−9.8	Carbonate type	Na–Cl–HCO_3
16	Hot spring	0.150	0.040	1.440	0.034	0.001	44.8	0.713521	−74	−9.8	Magnesium sulfate subtype	Na–Ca–SO_4–Cl–HCO_3
17	Hot spring	0.250	0.750	2.350	0.140	0.015	34.1	0.711046	−76	−9.5	Sodium sulfate subtype	Na–Ca–SO_4–Cl
18	Saline spring	10.500	4.380	22.000	1.940	0.075	21.7	–	–	–	Chloride type	Na–Cl
19	Saline spring	10.300	4.410	21.700	1.950	0.076	20.9	–	–	–	Chloride type	Na–Cl
20	Hot spring	0.170	0.100	2.970	0.100	0.005	21.1	0.708387	−60	−7.8	Chloride type	Na–Ca–Cl–HCO_3
21	Hot spring	2.160	0.920	10.900	0.940	0.038	43.6	0.710954	−59	−7.8	Chloride type	Na–Cl

[a] T_{sring} represents outlet temperature of spring water.
[b] T_r represents the calculated credible reservoir temperature.
[c] Valyashko's classification.
[d] Schukalev's classification.

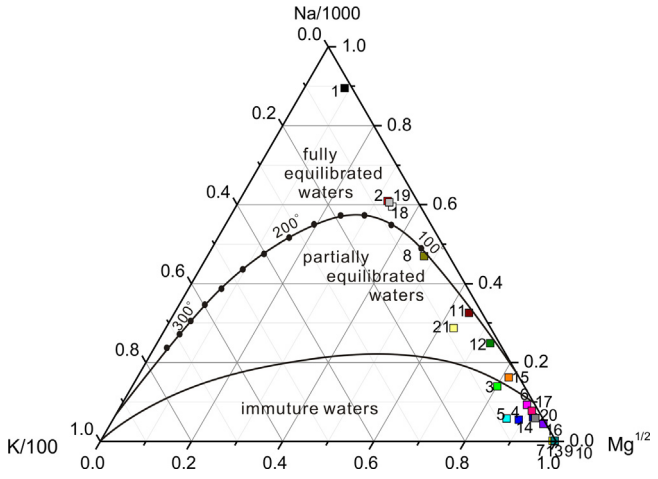

Fig. 6. Distribution of spring waters from the study area in the Na–K–Mg triangular diagram (adapted from Giggenbach, 1988).

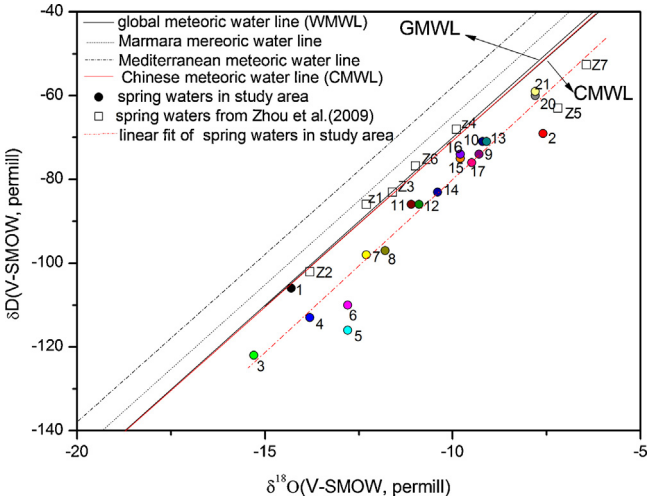

Fig. 7. Distribution of spring waters from the Lanping–Simao Basin, northern Laos, and other sites in Yunnan in the $\delta^{18}O$–δD diagram. Data for Yanjing are from Qian (2007). Data for Z1–Z7 are from Zhou et al. (2009); the corresponding sampling sites are shown in Fig. 1.

If $\theta_{NaK} > \theta_{NaKCa} > \theta_{KMg} > \theta_{SiO_2}$ and $T_{spring} > 40\,^{\circ}C$,

then $T_r = \theta_{KMg}$.

According to those rules mentioned above, the Na–K thermometer is only used for three hot spring samples (Nos. 6, 15 and 16), the silica thermometer is used for the other spring samples, and the other two thermometers are excluded in this study.

The Na–K–$Mg^{1/2}$ ternary diagram was proposed by Giggenbach (1988) as a method of identifying thermal waters that are suitable for the estimation of reservoir temperature by the application of solute geothermometers. This method has been used in some previous studies (Yousafzai et al., 2010; Sanliyuksel and Baba, 2011; Makni et al., 2013; Liu et al., 2015). As shown in Fig. 6, most saline spring samples (except sample No. 8) in this study fall in the fully equilibrated water zone, cold spring samples fall in the immature water zone (close to the $Mg^{1/2}$-end-member), while hot spring samples fall in both immature water zone and partly equilibrated water zone. This indicates that water–rock interactions have not reached equilibrium for hot springs and cold springs in the study area. For anion geothermometers are not suitable for immature waters (Giggenbach, 1988), the T_r values of Nos. 6 and 16 spring samples calculated with the Na–K geothermometer are not given (Table 1).

As listed in Table 1, the calculated credible reservoir temperature (T_r) of hot spring waters, cold spring waters, and saline spring waters are in the ranges 65.5–144.1, 37.8–64.4, and 65.1–109.0 °C, respectively. If the influence of cold water was deducted, the real reservoir temperatures should be much higher.

The geothermal gradients in the Lanping–Simao Basin are between 20 and 30 °C/km (Yuan et al., 2006). Using 30 °C/km for hot springs and 20 °C/km for cold springs and saline springs, the ranges of circulation depth for hot springs, cold springs, and saline springs are 848.9–2833.8, 1140.5–2468.7, and 2505.3–4701.6 m, respectively.

4.3. Oxygen and hydrogen isotopic characteristics

The relationship between $\delta^{18}O$ and δD values is plotted in Fig. 7, which also shows the worldwide meteoric line ($\delta D = 8 \times \delta^{18}O + 10$; Craig, 1961), Marmara meteoric water line ($\delta D = 8 \times \delta^{18}O + 15$; Eisenlohr, 1997), Mediterranean meteoric water line ($\delta D = 8 \times \delta^{18}O + 22$; Gat and Carmi, 1970), and Chinese meteoric line ($\delta D = 7.9 \times \delta^{18}O + 8.2$) (Zheng et al., 1983). Positive shifts in $\delta^{18}O$ values are related to $\delta^{18}O$ exchange between deeply circulating meteoric waters and host rocks in geothermal systems. The degree of the shift depends on the reservoir temperature, residence time, and water–rock interaction (Truesdell and Hulston, 1980). According to Zhou et al. (2009), thermal groundwater of low to moderate temperature in China does not show a positive oxygen shift; in Southwestern China, only thermal waters in western Yunnan (Tengchong and Ruili, corresponding to samples No. Z5 and No. Z7 in Fig. 7) and Tibet show a slight oxygen shift. The results of this study show that a slight positive oxygen shift can be observed in most spring waters of the Lanping–Simao Basin. This indicates that oxygen and hydrogen isotope compositions in the Lanping–Simao Basin are primarily controlled by meteoric waters and are also influenced by $\delta^{18}O$ exchange to some extent.

Isotopic latitude and altitude effects are observed in the study area. In general, spring waters from the northern part of the basin show obviously lower $\delta^{18}O$ and D values than those from the southern part of the basin; both $\delta^{18}O$ and D values correlate well with latitude, with calculated regression lines $Y = -0.07848X + 17.45252$ ($n = 19$, $R^2 = 0.60157$) and $Y = -0.60405X + 17.70128$ ($n = 19$, $R^2 = 0.48778$), respectively (Fig. 8c and d). The relationships between $\delta^{18}O$ and D values and altitude can be expressed by the regression lines $Y = -26.74194X - 831.59496$ ($n = 19$, $R^2 = 0.63814$) and $Y = -211.9886X - 813.40329$ ($n = 19$, $R^2 = 0.55315$), respectively (Fig. 8a and b).

4.4. Strontium isotope hydrogeology

Strontium can be found in easily measurable quantities in a wide variety of rocks and is a good tracer of the source rock of the chemical constituents in water. It is soluble in aqueous solution as +2 ion and is geochemically very similar to Ca. The $^{87}Sr/^{86}Sr$ ratio has been extensively used to trace salts resources, groundwater movements, and water–rock interactions (Wang et al., 2009). Sr isotope studies of waters have highlighted that differences in the $^{87}Sr/^{86}Sr$ ratio and Sr concentration are primarily caused by mixing of waters of various origins with specific isotopic and chemical characteristics (Nisi et al., 2006).

The strontium isotope ratio of water is strictly controlled by rock–water interactions. In a very general way, the $^{87}Sr/^{86}Sr$ ratio of water reflects the mineralogy of the rocks with which the water has been in contact. Commonly the radioisotope ^{87}Sr is more enriched

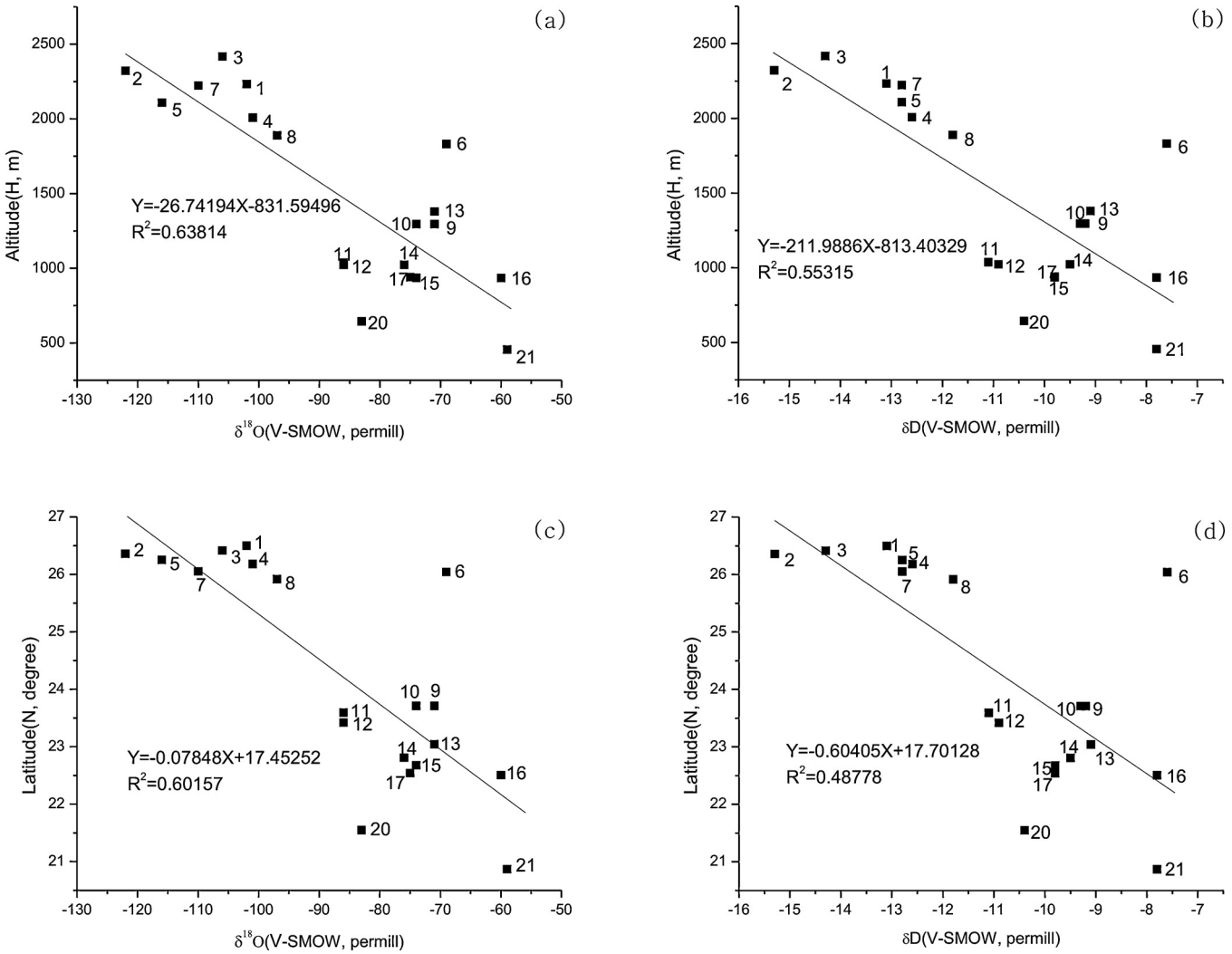

Fig. 8. Relationships between (a) $\delta^{18}O$ and altitude, (b) δD and altitude, (c) $\delta^{18}O$ and latitude, and (d) δD and latitude in spring waters from the Lanping–Simao Basin and northern Laos.

in older rocks, for instance, very old silicate rocks have the highest $^{87}Sr/^{86}Sr$ ratios (much higher than 0.730) (Goldstein and Jacobsen, 1987) and young volcanic rocks have the lowest $^{87}Sr/^{86}Sr$ ratios (between 0.703 and 0.706) (Chaudhuri and Clauer, 1992). In studies of river water, two end-members of $^{87}Sr/^{86}Sr$ ratios and Sr contents are usually used: the silicate end-member (high $^{87}Sr/^{86}Sr$ and low Sr content) and the carbonate end-member (low $^{87}Sr/^{86}Sr$ and high Sr content). In addition, continental silica rocks usually have higher $^{87}Sr/^{86}Sr$ ratios (>0.710) and lower Sr contents; basalts and alkaline rocks have lower $^{87}Sr/^{86}Sr$ ratios (<0.710) and higher Sr contents (Wang et al., 2001). In a saline basin, waters with higher $^{87}Sr/^{86}Sr$ ratios are usually related to leaching and dissolution of meteoric water at the earth's surface, i.e., surface water, and waters with lower $^{87}Sr/^{86}Sr$ ratios are usually related to deep circulation of meteoric waters to the deep basin or upper mantle (Wang et al., 2001), i.e., deep groundwater.

Sr isotopic compositions show varied sources of spring waters in the study area. Binary diagrams of $^{87}Sr/^{86}Sr$ versus 1/Sr, $^{87}Sr/^{86}Sr$ versus Sr/Ca (μM/mM), strontium versus calcium, and strontium versus sulfate of water samples from the Lanping–Simao Basin and northern Laos are shown in Fig. 9. The saline springs with higher TDS values, higher Sr contents (8.890–48.900 mg/L), and lower $^{87}Sr/^{86}Sr$ ratios (0.7094–0.7098) demonstrate the derivation of Sr from deep circulation of meteoric waters through evaporites (Fig. 9a and Table 1). Two cold springs (Nos. 7 and 13) with the lowest $^{87}Sr/^{86}Sr$ ratios (0.7080 and 0.7078) may be related to deep circulation of meteoric waters through less radiogenic rocks (evaporites or carbonate rocks); two other cold springs (Nos. 9 and 10) with the lowest Sr contents may have been caused by dilution of meteoric water, taking into account that the salinities are the lowest and the $^{87}Sr/^{86}Sr$ ratios are slightly higher than 0.710. Hot springs may be derived from varied sources, with $^{87}Sr/^{86}Sr$ ratios ranging from 0.7084 to 0.7149 and Sr contents varying between 0.35 and 12.4 mg/L. The Sr in four hot spring samples (Nos. 5, 11, 12, and 20) with $^{87}Sr/^{86}Sr$ ratios lower than 0.710 is mainly derived from deep circulation of meteoric water, among which two (No. 11 and 12) with lower $^{87}Sr/^{86}Sr$ values and higher Sr contents and salinities indicate that the main part of the dissolved Sr may be derived from less radiogenic rocks, such as evaporites and carbonates. In No. 3 hot spring, which has the highest $^{87}Sr/^{86}Sr$ value, Sr may be mainly derived from more radiogenic rocks (silicates). The higher $^{87}Sr/^{86}Sr$ ratios of other hot spring waters (Nos. 4, 6, 14, and 16) also indicate more radiogenic sources of Sr.

According to Odum (1957), the Sr/Ca ratio (μM/mM) of fresh water varies between 0.5 (water from regions with consolidated carbonate rocks) and 5 or more (water from volcanic areas). The average Sr/Ca ratio of representative rivers of the world is 2.2 (Odum, 1951). In the study area, the Sr/Ca ratios for saline springs

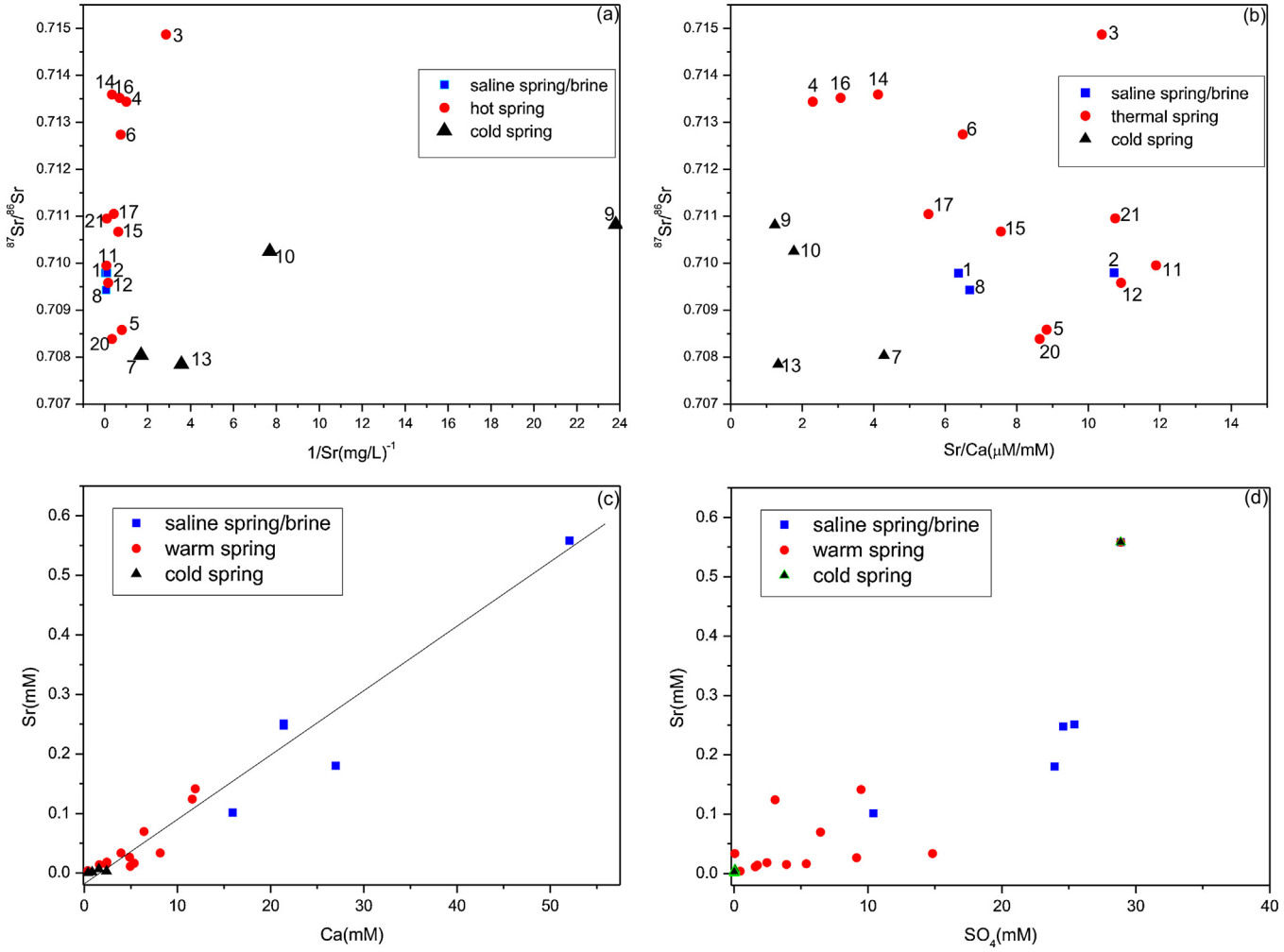

Fig. 9. Binary diagrams of (a) $^{87}Sr/^{86}Sr$ versus 1/Sr, (b) $^{87}Sr/^{86}Sr$ versus Sr/Ca (μM/mM), (c) strontium versus calcium, and (d) strontium versus sulfate of water samples from the Lanping–Simao Basin and northern Laos. There is a strong relation (R^2 = 0.9462) between Sr and Ca in water samples from the study area; Sr and SO_4^{2-} also correlate well (R^2 = 0.7191).

and most hot springs are greater than 5; some (Nos. 2, 3, 11, 12 and 21) have ratios even higher than the value for sea water (9.23) (Fig. 9b). This indicates that the strontium isotopic compositions of saline spring waters and most hot spring waters in the study area are influenced by volcanic rocks. The relatively lower Sr/Ca ratios of cold springs are accounted for by dilution of meteoric water and weaker water–rock interaction as a result of lower temperature.

There is a very strong relation between the concentrations of Sr^{2+} and Ca^{2+}, with a calculated regression line $Y = 0.0105X - 0.015$ (n = 21, R^2 = 0.9462) (Fig. 9c). Sr^{2+} and SO_4^{2-} correlate well, with a calculated regression line $Y = 0.0118X - 0.008$ (n = 21, R^2 = 0.7191) (Fig. 9d). This indicates that quite a significant portion of the Sr^{2+} in spring waters of the Lanping–Simao Basin is derived from dissolution of carbonates and evaporite minerals, which is consistent with the lithologic characteristics of the area.

4.5. Helium and neon isotopic compositions

The He isotope method is very effective in determining whether mantle-derived components are involved in crustal fluids. An early study by Hu et al. (1998) indicated that He isotopes from fluid inclusions in pyrites show no effect of mantle-derived He on the ore-forming fluid of the Jinding Ore Deposit, with R/R_a ratios in the range 0.03–0.06. Another study by Xue et al. (2003) showed that the main ore-forming fluid inclusions in the Jinding and Baiyangping ore deposits (the latter is another Pb–Zn ore deposit in Lanping County, about 30 km to the north of the Jinding Ore Deposit, Fig. 3) contain a small proportion of mantle-derived He, with R/R_a ratios of 0.19–0.82 (Jinding) and 0.71–1.97 (Baiyangping).

In this study, the $^3He/^4He$ ratios of gases escaping from springs in the study area (including the sample from northern Laos, G11) range from 0.034 R_a to 1.043 R_a (Table 2), showing that for almost all springs much of the He is derived from the crust, except for sample No. G7 (Fig. 10), which may show a mantle–crust mixed source of He. Comparing with much mantle-derived He in volcanic areas of Tengchong (Shangguan et al., 1997; 2000), where faults are connected with the magma chamber (Zhao et al., 2006), the wide distribution of crust-derived He reveal that faults in the Lanping–Simao Basin and northern Laos may not descend to the upper mantle.

On the basis of a ternary model of mixed gases, the proportions of air-derived He (A), crust-derived He (C), and mantle-derived He (M) can be calculated according to Eqs. (A.5)–(A.7) (Sano and Wakita, 1985; Zhao, 2008): the results are listed in Table 2. If the detected R/R_a ratios (Table 2) for gas samples from springs in the study area are corrected according to Eqs. (A.8) and (A.9) (Craig et al., 1978), in order to eliminate the hybridism of air, the corrected proportions of crust-derived He (C_c) and mantle-derived He (M_c) can be calculated on the basis of the binary model of mixed gases (Eqs. (A.10) and (A.11)). As shown in Table 2, crust-derived

Table 2
Contents and isotope compositions helium and neon in spring waters of the study area.

Sample No.	T_{spring} (°C)	^{4}He(E-4) (V/V)	^{20}Ne(E-4) (V/V)	^{4}He/^{20}Ne	R/R_a[a]	$(R/R_a)_c$[b]	A (%)	C (%)	M (%)	C_c (%)	M_c (%)
G1	51	2.92	0.0280	104.3125	0.03404	0.03109	0.27	99.46	0.26	99.85	0.15
G2	40	0.68	0.0339	20.2144	0.40144	0.39187	1.54	93.67	4.79	96.57	3.43
G3	81	4.44	0.0221	200.7111	0.15161	0.15026	0.13	98.09	1.78	98.77	1.23
G4	<20	0.09	0.0267	3.3784	0.61579	0.57587	9.38	84.09	6.53	94.89	5.11
G5	71	10.87	0.0399	272.2395	0.03959	0.12272	0.09	99.56	0.36	99.79	0.21
G6	50	13.47	0.0378	356.1476	0.11661	0.11582	0.06	98.60	1.34	99.08	0.92
G7	48	3.76	0.0128	293.5527	1.04321	1.04326	0.08	86.77	13.15	90.64	9.36
G8	60	0.19	0.0378	356.1476	0.64845	0.64814	0.06	91.82	8.12	94.24	5.76
G9	40	3.79	0.0249	151.8963	0.07743	0.07549	0.18	98.99	0.83	99.45	0.55
G10	<20	0.66	0.0351	18.7715	0.28968	0.27744	1.66	94.99	3.35	97.61	2.39
G11	66	8.17	0.0363	225.0518	0.22770	0.22661	0.11	97.14	2.75	98.07	1.93

[a] R represents the ^{3}He/^{4}He ratio of gas samples; R_a represents the ^{3}He/^{4}He ratio of the air; R/R_a corresponds to ^{3}He/^{4}He(R_a) in Fig. 10.
[b] "c" means "corrected".

He accounts for 90.64%–99.85% of total He.

$$(^3\mathrm{He}/^4\mathrm{He}) = (^3\mathrm{He}/^4\mathrm{He})_{air} \cdot A + (^3\mathrm{He}/^4\mathrm{He})_{mantle} \cdot M + (^3\mathrm{He}/^4\mathrm{He})_{crust} \cdot C \quad (A.5)$$

$$1/(^4\mathrm{He}/^{20}\mathrm{Ne}) = A/(^4\mathrm{He}/^{20}\mathrm{Ne})_{air} + M/(^4\mathrm{He}/^{20}\mathrm{Ne})_{mantle} + C/(^4\mathrm{He}/^{20}\mathrm{Ne})_{crust} \quad (A.6)$$

$$A + M + C = 1 \quad (A.7)$$

$$(R/R_a)_c = [(R/R_a) \cdot X - 1]/(X - 1) \quad (A.8)$$

$$X = (^4\mathrm{He}/^{20}\mathrm{Ne})/(^4\mathrm{He}/^{20}\mathrm{Ne})_{air} \quad (A.9)$$

$$(^3\mathrm{He}/^4\mathrm{He})_c = (^3\mathrm{He}/^4\mathrm{He})_{mantle} \cdot M_c + (^3\mathrm{He}/^4\mathrm{He})_{crust} \cdot C_c \quad (A.10)$$

$$M_c + C_c = 1 \quad (A.11)$$

$(^3\mathrm{He}/^4\mathrm{He})_{air} = 1.4 \times 10^{-6}$, $(^4\mathrm{He}/^{20}\mathrm{Ne})_{air} = 0.318$;
$(^3\mathrm{He}/^4\mathrm{He})_{mantle} = 1.1 \times 10^{-5}$, $(^4\mathrm{He}/^{20}\mathrm{Ne})_{mantle} = 1000$;
$(^3\mathrm{He}/^4\mathrm{He})_{crust} = 1.5 \times 10^{-8}$, $(^4\mathrm{He}/^{20}\mathrm{Ne})_{crust} = 1000$.

5. Discussion

5.1. Affinities and disaffinities of the Lanping–Simao Basin with surrounding areas

Geothermal Ca–Cl-type waters exist in many tectonically active closed basins, such as the Qaidam Basin and Tarim Basin, China (Lowenstein and Risacher, 2009; Bo et al., 2013), where faults offer potential pathways for upward movement of these waters. As shown in Fig. 11, the data points for one saline spring (No. 1) and two hot springs (Nos. 20 and 21) from the study area fall in the Ca–Cl field. Data points of other four saline springs (Nos. 2, 8, 18, and 19) and some hot springs (Nos. 11, 12, 14, 16, and 17) in the study area fall in the Cl–SO_4 field. Some springs (Nos. 8 and 11) plot near the chemical divide (the line from calcite to gypsum/anhydrite), which may indicate the addition of meteoric water to Ca–Cl-type brines (Lowenstein and Risacher, 2009). Therefore, saline springs and most hot springs of the study area are closely related to Ca–Cl-type brines. Furthermore, the hot springs of Yanjing (Qian, 2007; Bo and Liu, 2012) show obvious recharge of Ca–Cl-type waters. It can be concluded that geothermal Ca–Cl-type waters occur from the north (Yanjing) to the south (No. 21, Muangla, northern Laos) of a long and narrow salt-bearing belt (Yanjing–Lanping–Simao–northern Laos), revealing that these areas share geochemical affinities. Cold springs and other hot springs (Nos. 3, 4, 5, 6, and 15) fall into the Na–HCO_3–SO_4 field, and this may reflect recharge from surface water (derived from meteoric water).

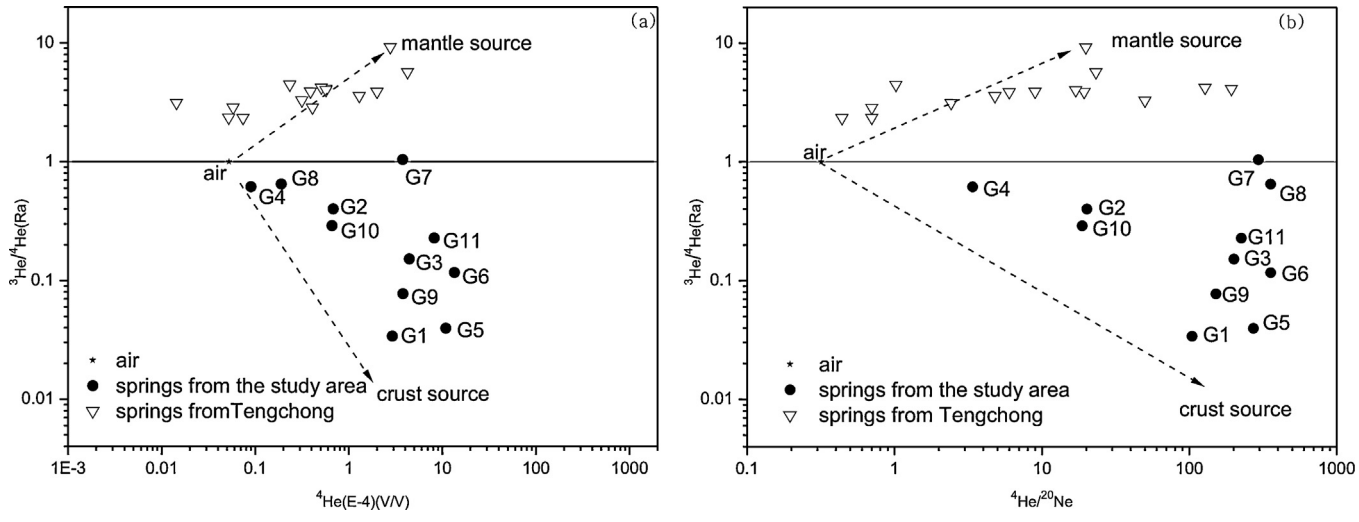

Fig. 10. Binary diagrams of (a) He versus ^{3}He/^{4}He(R_a) and (b) ^{4}He/^{20}Ne versus ^{3}He/^{4}He(R_a) of gases escaping from springs in the Lanping–Simao Basin, northern Laos, and Rehai. Data for Rehai, Tengchong, are from Shangguan et al. (1997).

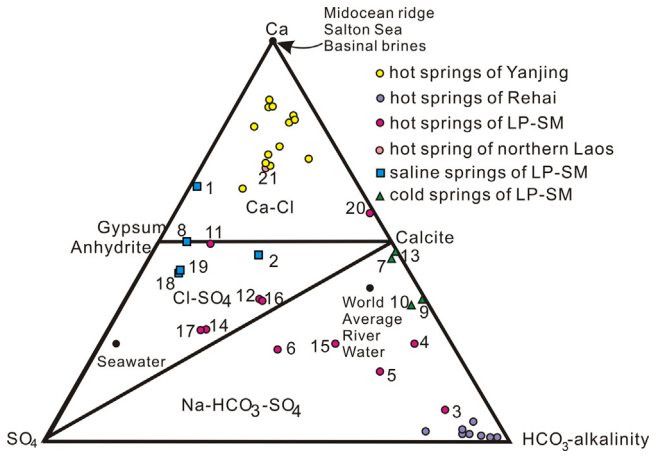

Fig. 11. Ternary $Ca–SO_4–HCO_3$ phase diagram showing the chemical compositions of spring waters in the Lanping–Simao Basin, northern Laos, Rehai, and Yanjing. Diagram modified from Lowenstein and Risacher (2009); data for Rehai and Yanjing are from Zhang et al. (1989) and Qian (2007), respectively.

From Fig. 11, data points for the hot springs in Rehai fall into the $Na–HCO_3–SO_4$ field very close to the HCO_3-end-member. This finding is closely related to the wide distribution of carbonate rocks in this area, verifying that the chemical characteristics of these waters are greatly different from the springs in the Lanping–Simao Basin, northern Laos, and Yanjing. Although both Langping–Simao Basin and Tengchong are located in western Yunnan, their formation lithologies, hydrochemical characteristics, and noble gas isotopic compositions are greatly different from each other, demonstrating that these two areas do not have geological affinities.

5.2. Circulation and evolution process of spring waters in the Lanping–Simao Basin

The chemical and isotopic characteristics of spring waters in the Lanping–Simao Basin are controlled by three main factors: the lithology of the host rocks (evaporites, carbonate rocks, silicate rocks, and volcanic rocks), heat source, and the recharge source of water. As stated in Section 4.2, the calculated circulation depths of springs are greatly different, ranging from 848.9 to 4701.6 m: saline springs circulate much deeper than hot and cold springs. The evolution process of spring waters in this area is concisely illustrated in Fig. 12. Meteoric water containing soluble mineral components (such as salts) leached from the host rocks circulates into the deep crust via faults. The water is then heated by the geothermal system and further water–rock interactions occur. Under certain tectonic and static pressures, spring waters ascend via faults to the surface of the earth, inevitably accompanied by mixing with surface water to some extent.

5.3. Chemical characteristics of springs and potassium prospecting

The different chemical characteristics of spring waters derived from meteoric water reflect the lithologies of the different strata that the waters flow through. Differences in the TDS values of springs may reveal an uneven distribution of evaporites, especially the Upper Cretaceous–Paleocene salt-bearing strata. From this viewpoint, the positions of buried salt-bearing strata may be identified using the distribution of saline springs. Though hundreds of saline springs were reported as flowing out in the Lanping–Simao Basin in the 1970s (Scientific Research Team for Potash Geology of Yunnan Geology Bureau, 1979), only a few of them can be found now because of strong late reformation of the earth's surface and human activities. On the basis of old data for these saline springs (more than 300 samples; Scientific Research Team for Potash Geology of Yunnan Geology Bureau, 1979), the contour maps of chemical components and ionic ratios have been drawn (Bo et al., 2014). Variations in the distributions of relevant elements and ionic ratios can help to identify geochemical anomalies in this area, providing useful information for further potassium prospecting.

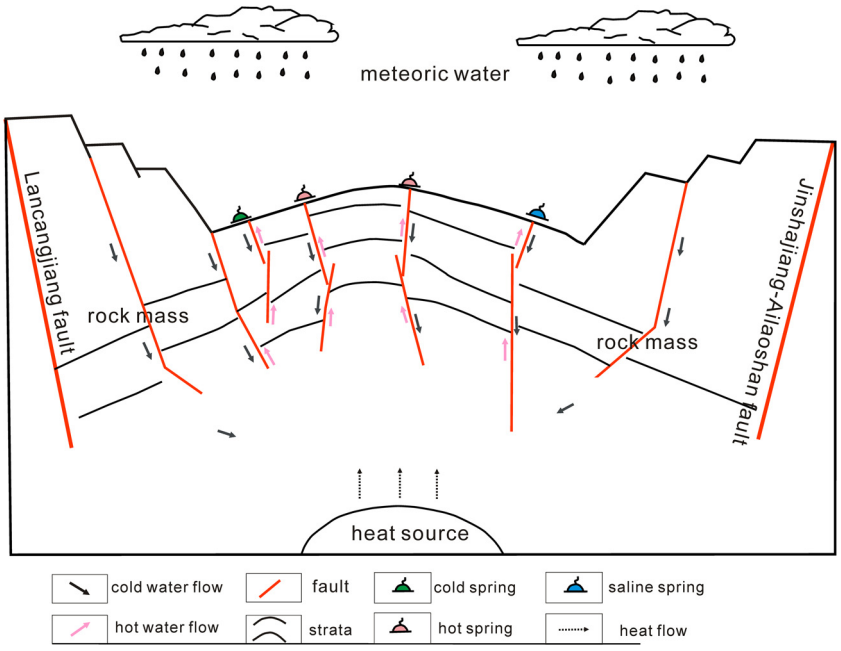

Fig. 12. Sketch map of the evolution process of springs in the Lanping–Simao Basin.

6. Conclusions

The chemical characteristics and isotopic compositions of spring waters in the Lanping–Simao Basin are mainly influenced by the rock lithology, the heat source of the geothermal system, and the recharge source of water. High TDS values of saline springs may be significantly related to the Upper Cretaceous–Paleocene salt-bearing strata. From the results of oxygen, hydrogen, and strontium isotopic analysis, spring waters of the Lanping–Simao Basin are mainly derived from leaching and deep circulation of meteoric water, and their strontium isotopic characteristics are greatly influenced by water–rock (evaporites, carbonate rocks, silicate rocks, and volcanic rocks) interactions.

On the basis of the calculated reservoir temperatures, the circulation depths of hot springs, cold springs and saline springs are predicted to be 848.9–2833.8, 1140.5–2468.7, and 2505.3–4701.6 m, respectively, i.e., saline springs circulate much deeper than hot and cold springs. Noble gas isotopic compositions show no obvious magma intrusion activity in the shallow crust of the study area, indicating that faults may not descend to the upper mantle and therefore water circulation may just be limited above the upper mantle.

Geothermal Ca–Cl-type waters are determined to be involved in the evolution of spring waters in the Lanping–Simao Basin, Yanjing and northern Laos, revealing that these areas are geochemically similar, whereas the noble gas isotopic compositions and hydrochemical characteristics demonstrate significant differences between these areas and Rehai, Tengchong, indicating that the Lanping–Simao Basin has geological affinities with Yanjing and northern Laos but not with the Tengchong Block.

Acknowledgements

Funding for this study was provided by the National Key Basic Research and Development Program (973 program, No. 2011CB403007) of the Chinese government. We are grateful to graduate students Dong Han and Ligang Qiu of China University of Geosciences (Beijing) for their help in sample collecting. We also would like to gratefully acknowledge the NRCGA (National Research Center for Geoanalysis) for their hard work in water sample analysis. In addition, Chao Gao and Fenglian Wang are thanked for their assistance with graph drawing.

References

814 Geological Team, Yunnan Bureau of Geology and Mineral Resources, 1994. Report on the Second Round Metallogenic Prospective Division for Potash Deposit of Yunnan Province, Fumin, Yunnan (in Chinese).

Bao, X.H., Qiu, Q.W., 2007. The development and utilization of wild birchleaf pear resources in Simao, Yunnan. For. By-Prod. Spec. China (5), 62–64 (in Chinese).

Bo, Y., Liu, C.L., 2012. Hydrochemistry of saline springs and clues for potash prospecting in Mangkang, Eastern Tibet. Miner. Depos. (Suppl.), 469–470 (in Chinese).

Bo, Y., Liu, C.L., Jiao, P.C., Chen, Y.Z., Cao, Y.T., 2013. Hydrochemical characteristics and controlling factors for waters' chemical composition in the Tarim Basin, western China. Chemie der Erde: Geochem. 73, 343–356.

Bo, Y., Liu, C.L., Zhao, Y.J., Wang, L.C., 2014. Hydrochemical characteristics and indicators for potassium exploration in Lanping–Simao Basin, Yunnan. Miner. Depos. 33 (5), 1031–1044 (in Chinese with English abstract).

Brook, C.A., Marina, R.H., Mabey, D.R., Swanson, J.R., Marianne, G., Moffler, L.J.P., 1979. Hydrothermal convection systems with reservoir temperature ≥90 °C. Assessment of geothermal resources of the United States – 1978. Geol. Surv. Circ. 790, 18–85.

Cao, Y.T., Liu, C.L., Jiao, P.C., Xuan, Z.Q., Chen, Y.Z., 2010. Relationship between surface copper mineralization and salt dome system in Kuqa Basin. Miner. Depos. 29 (3), 553–562 (in Chinese with English abstract).

Chaudhuri, S., Clauer, N., 1992. Isotopic Compositions of Dissolved Strontium and Neodymium in Continental Surface and Shallow Subsurface Waters. Isotopic Signatures and Sedimentary Records – Lecture Notes in Earth Sciences, vol. 43. Springer Verlag, Berlin, Heidelberg, pp. 467–495.

Coleman, M.L., Shepherd, T.J., Durham, J.J., Rouse, J.E., Moore, G.R., 1982. Reduction of water with zinc for hydrogen isotope analysis. Anal. Chem. 54, 993–995.

Craig, H., 1961. Isotopic variations in meteoric waters. Science 133, 1702–1708.

Craig, H., Lupton, J.E., Horibe, Y., 1978. A mantle helium component in Circum–Pacific Volcanic gases: Hakone, the Marianas and Mt. Lassen. In: Alexander Jr., E.C., Ozima, M. (Eds.), Terrestrial Rare Gases. Japan Sci. Sot. Press, Tokyo, pp. 3–16.

Eisenlohr, T., 1997. In: Schindler, C., Pfister, M. (Eds.), The Thermal Springs of the Armutlu Peninsula (NW Turkey) and Their Relationship to Geology and Tectonics in Active Tectonics of Northwestern Anatolia – The Marmara Poly Project. vdf Hochschulverlag AG an der ETH Zurich, pp. 197–228.

EPA, 2004. 2004 Edition of the Drinking Water Standards and Health Advisories. EPA 822-R-04-005. Office of Water, Environmental Protection Agency of the United States, Washington, DC.

Epstein, S., Mayeda, T.K., 1953. Variation of 18O content of waters from natural sources. Geochim. Cosmochim. Acta. 4, 213–224.

Fournier, R.O., 1979. Geochemical and hydrologic considerations and the use of enthalpy–chloride diagrams in the prediction of underground conditions in hot-spring systems. J. Volcanol. Geotherm. Res. 5, 1–6.

Fournier, R.O., 1981. Application of water geochemistry to geothermal exploration and reservoir engineering. In: Rybach, L., Muffler, L.J.P. (Eds.), Geothermal Systems: Principles and Case Histories. John Wiley and Sons Ltd., New York, pp. 109–143.

Gao, Q.W., Fan, S.Q., 1992. Geochemical characteristics of geothermal fluid in the active area of the Tengchong modern volcanoes. J. Xian Coll. Geol. 14 (3), 40–44 (in Chinese with English abstract).

Gat, J.R., Carmi, I., 1970. Evolution of the isotopic composition of atmospheric waters in the Mediterranean Sea area. J. Geophys. Res. 75, 3039–3048.

Giggenbach, W.F., 1988. Geothermal solute equilibria. Deviation of Na–K–Mg–Ca geoindicators. Geochim. Cosmochim. Acta 52, 2749–2765.

Goldstein, S.J., Jacobsen, S.B., 1987. The Nd and Sr isotopic systematics of river-water dissolved material: implications for the sources of Nd and Sr in seawater. Chem. Geol. (Isotype Geosci. Sect.) 66, 245–272.

Guo, F.X., 1986. Three salt-bearing belts and three salt-genesis periods from the Late cretaceous to the Eocene in Lanping–Simao Region, western Yunnan. Sci. Geol. Sin. 2, 161–169 (in Chinese with English abstract).

He, S.P., Li, R.S., Wang, C., Zhang, H.F., Ji, W.H., Yu, P.S., Gu, P.Y., Shi, C., 2011. Discovery of ~4.0 Ga detrital zircons in the Changdu Block, North Qiangtang, Tibetan Plateau. Chin. Sci. Bull. 56 (7), 647–658 (in Chinese with English abstract).

Hu, R.Z., Turner, G., Burnard, P.G., Zhong, H., 1998. Helium and argon isotopic geochemistry of Jinding surperlarge Pb–Zn deposit. Sci. China (Ser. D) 41 (4), 442–448.

Lanping Bai and Pumi Autonomous County Party Committee and Government, 2005. Agricultural Development Plan of Lanping Bai and Pumi Autonomous County (in Chinese).

Liu, H., Zhang, G.P., Jin, Z.S., Liu, C.Q., Han, G.L., Li, L., 2009. Geochemical characteristics of geothermal fluid in Tengchong Area, Yunnan Province, China. Acta Mineral. Sci. 29 (4), 496–501 (in Chinese with English abstract).

Lowenstein, T.K., Risacher, F., 2009. Closed basin brine evolution and the influence of Ca–Cl inflow waters: Death Valley and Bristol Dry Lake California, Qaidam Basin, China, and Salar de Atacama, Chile. Aquat. Geochem. 15, 71–94.

Liu, Y.P., Zhou, X., Deng, Z.J., Fang, B., Sutomu, Y., Zhao, J.B., Wang, X.C., 2015. Geothermics 53, 38–45.

MGMR, 1983. Hydrogeological Manual, Hydrogeological Engineering and Geological Technique Research Team, Ministry of Geology and Mineral Resources, The People's Republic of China. Geology Publishing House, Beijing, pp. 105–108 (in Chinese).

Makni, J., Bouri, S., Dhia, H.B., 2013. Hydrochemistry and geothermometry of thermal groundwater of southeastern Tunisia (Gabes region). Arab. J. Geosci. 6, 2673–2683.

Metcalfe, I., 2013. Gondwana dispersion and Asian accretion: tectonic and palaeogeographic evolution of eastern Tethys. J. Asian Earth Sci., http://dx.doi.org/10.1016/j.jseaes.2012.12.020

MGMR, 1987. Regulations for Water Sampling, Preservation and Determination, Ministry of Geology and Mineral Resources, the People's Republic of China. Geology Publishing House, Beijing (in Chinese).

Nisi, B., Vaselli, O., Buccianti, A., Perini, G., Minissale, A., Montegrossi, G., Tassi, F., 2006. Strontium isotope composition of the Arno River Valley waters (Tuscany Italy) as a natural tracer of water–rock interaction and mixing processes. Chin. J. Geochem. 25 (S1), 273.

Odum, H.T., 1951. The stability of the world strontium cycle. Science 114, 407–411.

Odum, H.T., 1957. Strontium in natural waters. Inst. Mar. Sci. 4, 22–37.

Qian, L., (Master Dissertation) 2007. Study on the Formation and Evolution Mechanisms of Underground Thermal Bittern in Yanjing County of Tibet. Chengdu University of Technology (in Chinese with English abstract).

Qian, Z.Q., Qu, Y.H., Liu, Q., 1994. Potash Deposit. Geological Publishing House, Beijing, pp. 148–243 (in Chinese).

Qu, Y.H., 1997. Geol. Chem. Miner. 19 (2), 81–84, 98 (in Chinese with English abstract).

Qu, Y.H., Yuan, P.Q., Shuai, K.Y., Zhang, Y., Cai, K.Q., Jia, S.Y., Chen, C.D., 1998. Potash-forming Rules and Prospect of Lower Tertiary in Lanping–Simao Basin Yunnan. Geological Publishing House, Beijing (in Chinese with English abstract).

Rybach, L., Muffler, L.J.P., 1981. Geothermal Systems: Principles and Case Histories. John Wiley and Sons Ltd.

Sanliyuksel, D., Baba, A., 2011. Hydrogeochemical and isotopic composition of a low-temperature geothermal source in northwest Turkey: case study of Kirkgecit geothermal area. Environ. Earth Sci. 62, 529–540.

Sano, Y., Wakita, H., 1985. Geographical distribution of $^{3}He/^{4}He$ ratios in Japan: implications for arc tectonics and incipient magmatism. J. Geophys. Res. 90, 8729–8741.

Scientific Research Team for Potash Geology of Yunnan Geology Bureau, 1979. Potassium Hydrochemical Research and Prediction on Potash Exploration in the Simao Basin, Yunan (in Chinese).
Shangguan, Z.G., Bai, C.H., Sun, M.L., 2000. Mantle-derived magmatic gas releasing features at the Rehai area, Tengchong County, Yunnan Province, China. Sci. China (Ser. D) 43 (2), 132–140.
Shangguan, Z.G., Deng, Y.Q., Dong, J.C., 1997. Material sources of escaped gases from Tianchi volcanic geothermal area, Changbai Mountains. Sci. China (Ser. D) 40 (4), 390–397.
Sun, Y.Z., Sun, S.Q., 1990. The structure paleohydrogeology and minerogenesis of Lanping–Simao Basin. J. Chengdu Coll. Geol. 17 (3), 102–111 (in Chinese with English abstract).
Tong, W., Zhang, M.T., 1989. Geothermal Springs in Tengchong. Science Press, Beijing (in Chinese).
Tornos, F., Heinrich, C.A., 2008. Shale basins, sulfur-deficient ore brines and the formation of exhalative base metal deposits. Chem. Geol. 247, 195–207.
Truesdell, A.H., 1975. Summary of section III: geochemical techniques in exploration. In: Proceedings UN Symposium on the Development and Utilization of Geothermal Resources, vol. 1, San Francisco, pp. 731–739.
Truesdell, A.H., Hulston, J.R., 1980. Isotopic evidence of environments of geothermal systems. In: Fritz, P., Fontes JCh (Eds.), Handbook of Environmental Isotope Geochemistry. The Terrestrial Environment, vol. 1. Elsevier, Amsterdam, pp. 179–226.
Valyashko, M.G., (F. Li, Trans.) 1965. Geochemical Formation Rules of Potash Deposition. China Industry Press, Beijing, 18 pp. (in Chinese).
Wang, M.L., Liu, C.L., Jiao, P.C., Han, W.T., Song, S.S., Chen, Y.Z., Yang, Z.C., Fan, W.D., Li, T.Q., Li, C.H., Feng, J.X., Chen, J.Z., Wang, X.M., Yu, Z.H., Li, Y.W., 2001. Saline Lake Potash Resources in the Lop Nur Xinjiang. Geological Publishing House, Beijing (in Chinese).
Wang, Y.S., Chen, J.S., Chen, L., 2009. Tracing groundwater with strontium isotopic compositions in the Hexi Corridor Basin, Northwestern China. Adv. Water Resour. Hydraul. Eng., 184–187 (in Chinese with English abstract).
Xue, C.J., Chen, Y.C., Wang, D.H., Yang, J.M., Yang, W.G., Zeng, R., 2003. Geology and isotopic composition of helium, neon, xenon and metallogenic age of the Jinding and Baiyangping ore deposits, northwest Yunnan, China. Sci. China (Ser. D) 46 (8), 789–800.
Ye, X.R., Tao, M.X., Yu, C.A., Zhang, M.J., 2007. Helium and neon isotopic compositions in the ophiolites from the Yarlung Zangbo River, Southwestern China: the formation from deep mantle. Sci. China (ser. D) 50, 801–812.
Yin, H.H., 1990. Deep processes and mantle–crust compound mineralization in the evolution of the Lanping–Simao Mesozoic–Cenozoic Diwa Basin in western Yunnan, China. Geotecton. Metallog. 14 (2), 113–124 (in Chinese with English abstract).
Yousafzai, A., Eckstein, Y., Dahl, P.S., 2010. Hydrochemical signatures of deep groundwater circulation in a part of the Himalayan foreland basin. Environ. Earth Sci. 59, 1079–1098.
Yuan, Y.S., Ma, Y.S., Hu, S.B., Guo, T.L., Fu, X.Y., 2006. Present-day geothermal characteristics in South China. Chin. J. Geophys. 49 (4), 1118–1125 (in Chinese with English abstract).
Zhang, Z.F., Liu, S.B., Zhao, F.S., 1989. Geochemistry of Hydrothermal Fluid in Tengchong. Geotherm in Tengchong County. Science Press, Beijing (in Chinese).
Zhao, C.P., (Doctoral Dissertation) 2008. Mantle-derived Helium Release Characteristics and Deep Magma Chamber Activities of Present Day in the Tengchong Volcanic Area. Institute of Geology, State Seismological Bureau (in Chinese with English abstract).
Zhao, C.P., Ran, H., Chen, K.H., 2006. Present-day magma chambers in Tengchong volcano area inferred from relative geothermal gradient. Acta Petrol. Sin. 22 (6), 1517–1528 (in Chinese with English abstract).
Zheng, S., Hou, F., Ni, B., 1983. Hydrogen and oxygen isotopic studies of meteoric water in China. Chin. Sci. Bull. 28, 801–806 (in Chinese).
Zhou, X., Fang, B., Zhou, H.Y., Li, J., Wang, Y., 2009. Isotopes of deuterium and oxygen-18 in thermal groundwater in China. Environ. Geol. 57, 1807–1814.
Zhou, Z.H., Xiang, C.Y., Yang, K.J., 2001. Petrological structure of the crust and upper mantle in Yunnan, China. Seismol. Geol. 23 (1), 69–78 (in Chinese with English abstract).
Zhu, C.Y., Xia, W.J., Yin, H.S., Wei, J.Y., 1997. The tectonic nature and evolution of Mesozoic Lanping–Simao Basin. J. Chengdu Univ. Technol. 24, 23–30 (in Chinese with English abstract).